Research Square

Preprints are preliminary reports that have not undergone peer review.
They should not be considered conclusive, used to inform clinical practice,
or referenced by the media as validated information.

Is the Cardiac Magnetic Resonance Cine Images Capable of Differentiating Between LVEF-preserved Light-chain Amyloidosis and Hypertrophic Cardiomyopathy? —the Value of Left Atrial Parameters

Jianyao Lu
Tongji Hospital of Tongji Medical College of Huazhong University of Science and Technology Department of Radiology

Wen Zhou
Tongji Hospital of Tongji Medical College of Huazhong University of Science and Technology Department of Radiology

Jinhan Qiao
Tongji Hospital of Tongji Medical College of Huazhong University of Science and Technology Department of Radiology

Peijun Zhao
Tongji Hospital of Tongji Medical College of Huazhong University of Science and Technology Department of Radiology

Lu Huang
Tongji Hospital of Tongji Medical College of Huazhong University of Science and Technology Department of Radiology

Dazhong Tang
Tongji Hospital of Tongji Medical College of Huazhong University of Science and Technology Department of Radiology

Liming Xia (✉ xialiming2017@outlook.com)
Tongji Hospital of Tongji Medical College of Huazhong University of Science and Technology
https://orcid.org/0000-0001-8481-3380

Research Article

Keywords: light-chain amyloidosis, hypertrophic cardiomyopathy, differential diagnosis, left atrial, cine images

Posted Date: August 31st, 2021

DOI: https://doi.org/10.21203/rs.3.rs-838399/v1

License: This work is licensed under a Creative Commons Attribution 4.0 International License.
Read Full License

Abstract

Purpose: Due to the limited application of late gadolinium enhancement (LGE) in patients with renal insufficiency and the lack of advanced mapping technique, non-invasively discriminating left ventricular ejection fraction (LVEF)-preserved light-chain amyloidosis (AL) from hypertrophic cardiomyopathy (HCM) with similar left ventricular (LV) hypertrophy was challenging. The aims of this study were to evaluate left atrial (LA) morphology and function in LVEF-preserved AL patients using CMR cine images and to investigate the ability of CMR-derived LA parameters in discriminating LVEF-preserved AL from HCM.

Methods and results: Thirty-eight confirmed LVEF-preserved AL patients and 38 HCM patients as well as 20 healthy controls were enrolled in this retrospective study. Morphological and functional parameters of LA and LV were measured in multi-plane cine images. Receiver operator characteristics curves were generated to estimate the discriminative ability of parameters. The LA active contractile function of AL and HCM patients were both significantly impaired compared to the control, and the impairment of AL patients was severer than that of HCM (all $P < 0.05$). In morphological aspect, thickened maximum atrial septal thickness (ASH_{max}) was found in AL group with regard to HCM and control. Combining ASH_{max} and LA functional parameters had excellent discriminative ability between AL and HCM (area under the curve [AUC] > 0.9).

Conclusions: The combination of ASH_{max} and LA function was able to perform accurately non-invasive differentiating diagnosis between AL and HCM patients in limited clinical condition, and it could helpfully complemented and extended the current AL diagnostic strategies.

Introduction

Cardiac amyloidosis (CA) was defined as insoluble amyloid fibrin deposited within the heart [1]. Light-chain (AL) amyloidosis was one of the most common types of CA [2]. All structures of the heart can be involved, that were, the myocardium, the coronary arteries, and the conducting system. CA patients initially manifested myocardial diastolic dysfunction, then stepwisely progressed to systolic dysfunction, abnormal electrical conduction, myocardial ischemia, and finally to congestive heart failure [3, 4].

The conventional view was that CA patients mainly demonstrated symmetrically concentric hypertrophy. In recent years, Pozo and colleagues [5] had reported that asymmetric left ventricular (LV) hypertrophy could be shown by up to 66.7% of AL patients. Both AL and hypertrophic cardiomyopathy (HCM) patients could demonstrate symmetric or asymmetric myocardial hypertrophy, this similar imaging feature might led to misdiagnosis. It was critical to precisely differentiate AL and HCM as the mortality of the two diseases were significantly different. The rapid disease progression of AL underscored the need for timely and accurate diagnosis and subsequently rapid initiation of therapies were allowed for.

Endocardial biopsy was the “golden standard” diagnostic method of AL, but it wasn’t routinely applied because of the invasive nature. Cardiac magnetic resonance (CMR), as a valuable tool with high temporal and spatial resolution as well as great ability for tissue characterization, was widely regarded as

the ”gold standard” for cardiac morphological and functional measurement, and was commonly used in suspicious AL patients’ evaluation [6, 7]. Late gadolinium enhancement (LGE) practically distinguished AL and HCM based upon specific LGE patterns: the characteristic LGE pattern of AL was diffuse subendocardial or transmural dust-like enhancement [8, 9], and that of HCM was patchy enhancement in hypertrophy segments [10]. However, the high prevalence of renal inadequacy [11] impeded the administration of contrast agents in AL patients, which narrowed the adaptable range of the contrast method. Advanced T1 mapping technique and deuterogenic extracellular volume fraction (ECV) were reported effective in distinguishing CA from other cardiomyopathies [12-14] while its prevalence was confined to the advancedness. CMR cine sequence was easily acquired and could perform reliable measurement of the cardiac morphology and function, which was available for any institution with MR scanner and could be used by a bigger crowd. Researches had shown that LV strain was capable of differentiating AL and HCM [15-17]. But CMR-derived strain parameters asked for extra post-processing software, so it was hardly be used in much of clinical condition.

It had previously been reported that the left atrial (LA) morphology and function of CA patients changed during disease process [18, 19], and it could differentiate diseases with similar hypertrophic features [20-22]. Therefore, LA manifestation may be a potential key point of AL diagnosis. However, study focused on whether the CMR-derived LA parameters could identify AL from HCM is still rare currently. The morphological parameters of LA including the left atrial volume (LAV) and maximum atrial septal thickness (ASH_{max}). The functional parameter was LA emptying fraction (LAEF), which consists of three parts: total function represented the global contractile function of LA; conduit function indicated the transmission of blood from LA to LV during early ventricular diastole; booster pump function referred to the active contraction of LA during late ventricular diastole.

In this study, we sought to investigate the ability of CMR-derived parameters in describing LA changes of LVEF-preserved AL patients and that in differentiating LVEF-preserved AL from HCM using conventional cine images.

Methods

Study population

We retrospectively enrolled 134 suspicious CA patients who obtained CMR assessment in our institution from January 2017 to February 2021 (Fig.1). Inclusion criteria were: (1) CMR indicated suspicious CA; and (2) peripheral tissue biopsy confirmed amyloidosis (kidney, subcutaneous fat, tongue, or bone marrow), demonstrating Congo red staining with typical birefringence under polarized light; and (3) immunofluorescence or immunohistochemistry showed positive light-chain staining.

And we also included 38 HCM patients as well as 20 healthy controls with matched sex and age who underwent CMR scanning from May 2018 to January 2020. HCM patients’ inclusion followed these

criteria: (1) normal LV cavity size with unexplained LV wall thickness ≥ 15 mm, or ≥ 13 mm with family history; and (2) without any other disease could lead to myocardial hypertrophy (such as amyloidosis, aortic stenosis, or Fabry disease) and (3) the myocardial thickness was not be explained by elevated blood pressure [23, 24]. Controls had neither history nor symptom of cardiovascular diseases with normal CMR findings.

Subjects were excluded if (1) with cardiac systolic dysfunction (LVEF ≥ 50%); or (2) atrial fibrillation was observed; or (3) mitral regurgitation occurred; or (4) CMR image quality was suboptimal for analysis. Clinical history, serological examinations, and electrocardiograph results of all subjects around the time of CMR scanning were collected.

The Institutional Ethics Committee approval of this study was obtained. The need for written informed consent was waived due to the retrospective design.

Cardiac magnetic resonance examination

All CMR examinations were performed on a 3T MR scanner (MAGNETOM Skyra, Siemens Healthcare) with supine position. Cine images were scanned using ECG-gated steady-state free precession during expiratory breath-holds. Standard 2-chamber, 3-chamber, 4-chamber, and short-axis views were acquired. The number of phases was 25. Typical image parameters were: field of view (FOV): 360 × 360mm^2; repetition time (TR): 37.7ms; time to echo (TE): 1.4ms; flip angle: 55°; slice thickness: 8mm; voxel size: 1.9 × 1.9 × 8.0mm^3; bandwidth: 965Hz / pixel.

Image analysis

Image analysis was performed offline using CVI42 (Circle Cardiovascular Imaging, Calgary, Canada). Patients' CMR data in random order were analysis by two double-blinded observers (J.Y.L. and W.Z., with 2 and 3 years of CMR experience respectively).

Maximum (at the phase of mitral valve opening), minimum (at the phase of mitral valve closing), and before-contraction (at the phase just before the active contraction of LA) LA contours were automatically detected and manually corrected on standard 4-chamber and 2-chamber views. The LA appendage and pulmonary veins were excluded (Fig.2a and 2b). The LAV was calculated using the biplane area-length method: LAV = 0.85 × A1 × A2 / L. A1 / A2 = the LA areas in the 4-chamber / 2-chamber views; L = the average of the maximal LA length (perpendicular to the mitral annulus plane) in the 4-chamber / 2-chamber views. LAV were indexed to the body surface area (BSA) when the statistical analysis was performed. The measurement of the ASH_{max} was taken perpendicular to the atrial septum during LA end-diastolic phase (Fig.2c). The LAEF were calculated by formulas supplied in Fig.2d. The LV cavity size and function were automatically sketched and computed by artificial intelligent algorithm in CVI42. If contours' error occurred, manual correction was carried out.

Observer variability analysis

The intra-observer variability assessment was conducted by a single observer (J.Y.L.). Twenty randomly selected scans recomputed LAV and ASH_{max}. The second analysis was performed 2 weeks apart from the first assessment. For inter-observer variability assessment, the same 20 scans were analyzed by a second blinded observer (W.Z.). Intra-class correlation coefficients (ICC) were ranked as follows: excellent > 0.90, good 0.75 - 0.90, moderate 0.50 - 0.75 and poor < 0.50 [25].

Statistical analysis

The statistical tests were performed using IBM SPSS Statistics for Windows, version 25.0 (IBM Corp, Armonk, NY, USA). We used the Pearson Chi-Square test or the Fisher's exact test for categorical variables and the one-way analysis of variance or the Kruskal-Wallis test for continuous variables, with post-hoc pairwise comparisons using the Bonferroni correction. Intra-observer and inter-observer agreement were assessed using ICC. Univariate and multivariate logistic regression analyses were performed and receiver operator characteristics (ROC) curves were generated to identify predictors of AL.

Results

Baseline characteristics

Thirty-eight AL, 38 HCM and 20 controls were finally included in our study. Their age and male gender proportion were similar (age, P = 0.354; sex, P = 0.334). The systolic blood pressure of HCM was higher than the other two groups (P = 0.02), but the diastolic blood pressure between subjects yielded no difference (P = 0.08). A higher proportion of patients with cardiac risk factors were found in the HCM group. Patients with AL had higher levels of high-sensitivity troponin I and N-terminal pro-brain natriuretic peptide, as well as severer impairment in renal function than patients with HCM (all $P \leq 0.001$). Other subjects' characteristics were shown in Table 1.

Morphology and function of left atrium and left ventricle

From Table 2, The ASH_{max} demonstrated a gradually decreasing trend among the three groups, with the highest in the AL group, the mid-range in HCM group, and the lowest in the control group (AL vs. HCM vs. Control, 7.5 ± 2.5 vs. 5.0 ± 1.2 vs. 4.2 ± 0.9, P < 0.001). The LAV indexes (LAVi) of AL patients were significantly increased than that of controls (all P < 0.05), there was no significant difference of LAVi between AL and HCM. The AL patients demonstrated significant impairment in total and booster LAEF than HCM and controls (all P < 0.05). Overall, these results indicated that the LA alternations were evident both in morphological and functional aspects between AL and HCM patients (Fig.3).

The end-diastolic maximum LV wall thickness was much the same between AL and HCM groups (16.1 [13.7, 18.6] vs. 17.3 [16.0, 18.7], P = 0.53). The LV end-diastolic and end-systole volume index decreased in HCM patients, that of AL patients and controls were similar. Although the LV function of AL patients was in a normal range (60.2 ± 7.2), it was significantly depressed when compared with that of

HCM patients and controls. A comparison between groups revealed that AL patients showed a markedly increase in LV myocardial mass than HCM and control.

Predictors of light-chain amyloidosis

The logistic regression and ROC analysis were carried out to assess whether CMR-derived LA parameters could be predictors of AL and to assess its ability in distinguishing AL from HCM. From Table 3 and Fig.4, we learned that most of LA morphological and functional parameters differentiated AL from HCM with good performance (area under the curve [AUC], 0.646 - 0.857). The single parameter performance of ASH_{max} was the best (AUC = 0.857, cutoff value = 6.319 mm, sensitivity = 84.2%, specificity = 84.5%, P < 0.001). It's a strong predictor of AL when combined ASH_{max} and $LAEF_{booster}$, with the AUC of 0.907, sensitivity of 86.8% and specificity of 84.5%. And the combination of ASH_{max} and $LAEF_{total}$ also performed excellently, with the AUC of 0.902, sensitivity of 86.8% and specificity of 86.2%.

Intra- and inter-observer variability

Table 4 showed ICC and 95% CI for variability assessments within single observer and between observers. Overall, the reproducibility of LAVi and ASH_{max} were excellent.

Discussion

The major findings of this study were (1) LVEF-preserved AL patients demonstrated worse LA function and more thickened ASH, comparing to HCM patients; (2) CMR-derived LA parameters were able to discriminate LVEF-preserved AL from HCM patients, particularly when combined ASH_{max} with $LAEF_{booster}$.

The LA morphological and functional remodeling of cardiomyopathies mostly contributed by mechanical stressors (volume / pressure overload) [26, 27]. Different stressors and duration time led to different manifestations of LA remodeling, which could be the reason of why AL and HCM showed different LA manifestations as our results reported. LV hypertrophy and reduced LV compliance, which were the common characteristics of AL and HCM, contributed to the increase of volume / pressure overload. In AL patients, the hypertrophy was mainly caused by amyloid deposition, while that of HCM patients were caused by myocardial fibrosis. Furthermore, amyloid deposited in LA myocardial interstitial had a direct influence on LA wall thickness and function [3]. The different mechanisms by which diseases produced their effects on LA led to markedly different manifestations of AL and HCM.

Our results promoted that CMR-derived LA parameters have powerful differentiating ability of amyloidosis, especially when combined ASH_{max} with LAEF. Although the diagnostic performance of ASH_{max} & $LAEF_{total}$ (AUC = 0.902) was not as good as that of ASH_{max} & $LAEF_{booster}$ (AUC = 0.907), we recommended the former combinative method more as it was easier to operate in clinical conditions. The difficulties of computing $LAEF_{booster}$ appeared when patients had severe LA contractile

dysfunction, since the phase of LA active contraction was hard to identify on cine images. But in that case, identifying the phases of maximum LAV and minimum LAV was much more simple. Therefore, the ASH_{max} & $LAEF_{total}$ combinative method with high accuracy and simplicity would be preferable for clinical differentiating diagnosis of AL and HCM.

The CMR-derived LA morphological and functional parameters provided huge diagnostic benefits for suspicious AL patients in limited clinical condition. And for those who in an applicable condition of LGE and mapping technique, LA parameters could play a complementary role in existing diagnostic strategies.

This study had several limitations. The mapping parameters were not included in this study which didn't allow direct comparison of the diagnostic performance between the LA parameters and mapping parameters. And the study population is limited to the inclusion criteria and AL prevalence, large-scale studies will be needed for further verification of the current result.

Conclusions

CMR-derived LA morphological and functional parameters are able to perform non-invasive differentiating diagnosis of AL and HCM, which played a complementary and extend role in the current diagnostic strategies. Numbers of patients with underdiagnosed AL may benefit from it as it provide valuable information for timely diagnosis in limited CMR conditions.

Declarations

Funding: This study was funded by the National Natural Science Foundation of China (NO. 81873889).

Conflicts of interest: Nothing to Disclose.

Availability of data and material: Datasets of this study are available upon request.

Code availability: Not applicable.

Authors' contributions: Study design were performed by Jianyao Lu, image analysis and statistical computation were performed by Jianyao Lu and Wen Zhou, the first draft of the manuscript was written by Jianyao Lu, suggestions for revision were proposed by Lu Huang, Liming Xia, Peijun Zhao and Jinhan Qiao, MR scanning was carried out by Dazhong Tang.

Ethics approval: According to the requirement of local institution, Institutional Review Board approval were waived of due to the retrospective design of the study.

Consent to participate: Written informed consent was waived of due to the retrospective design of the study.

Consent for publication: All authors agree to publish the article.

Acknowledgments: We would like to acknowledge hiplot.com.cn and www.processon.com for assistance regarding illustrations.

References

1. Kittleson MM, Maurer MS, Ambardekar AV, Bullock-Palmer RP, Chang PP, Eisen HJ et al. Cardiac Amyloidosis: Evolving Diagnosis and Management: A Scientific Statement From the American Heart Association. CIRCULATION. 2020 2020-07-07;142(1)
2. Kitaoka H, Izumi C, Izumiya Y, Inomata T, Ueda M, Kubo T et al. JCS 2020 Guideline on Diagnosis and Treatment of Cardiac Amyloidosis. CIRC J. 2020 2020-08-25;84(9):1610–1671
3. Wechalekar AD, Gillmore JD, Hawkins PN (2016) Systemic amyloidosis 387(10038):2641–2654
4. Nicol M, Baudet M, Brun S, Harel S, Royer B, Vignon M et al. Diagnostic score of cardiac involvement in AL amyloidosis. European Heart Journal - Cardiovascular Imaging. 2020 2020-05-01;21(5):542–548
5. Pozo E, Kanwar A, Deochand R, Castellano JM, Naib T, Pazos-López P et al (2014) Cardiac magnetic resonance evaluation of left ventricular remodelling distribution in cardiac amyloidosis. Heart 100(21):1688–1695 2014-01-01
6. Alicia Maria Maceira JJSK, Perugini IHMN, Pennell HADJ. Cardiovascular magnetic resonance in cardiac amyloidosis. CIRCULATION.;111(2):186–193
7. Mekinian A, Lions C, Leleu X, Duhamel A, Lamblin N, Coiteux V et al. Prognosis assessment of cardiac involvement in systemic AL amyloidosis by magnetic resonance imaging. AM J MED. [Comparative Study; Journal Article]. 2010 2010-09-01;123(9):864–868
8. Vogelsberg H, Mahrholdt H, Deluigi CC, Yilmaz A, Kispert EM, Greulich S et al (2008) Cardiovascular Magnetic Resonance in Clinically Suspected Cardiac Amyloidosis. J AM COLL CARDIOL 51(10):1022–1030
9. Chacko L, Martone R, Cappelli F, Fontana M. Cardiac Amyloidosis: Updates in Imaging. CURR CARDIOL REP. [Journal Article; Research Support, Non-U.S. Gov't; Review]. 2019 2019-08-02;21(9):108
10. Neubauer S, Kolm P, Ho CY, Kwong RY, Desai MY, Dolman SF et al (2019) Distinct Subgroups in Hypertrophic Cardiomyopathy in the NHLBI HCM Registry. J AM COLL CARDIOL 74(19):2333–2345
11. Merlini G, Dispenzieri A, Sanchorawala V, Schoenland SO, Palladini G, Hawkins PN et al (2018) Systemic immunoglobulin light chain amyloidosis. NAT REV DIS PRIMERS [Article] 4(1):38
12. Baggiano A, Boldrini M, Martinez-Naharro A, Kotecha T, Petrie A, Rezk T et al. Noncontrast Magnetic Resonance for the Diagnosis of Cardiac Amyloidosis. JACC. Cardiovascular imaging. 2020 2020-01-01;13(1):69–80
13. Haaf P, Garg P, Messroghli DR, Broadbent DA, Greenwood JP, Plein S. Cardiac T1 Mapping and Extracellular Volume (ECV) in clinical practice: a comprehensive review. J CARDIOVASC MAGN R.

2016 2016-01-01;18(1):89

14. Chatzantonis G, Bietenbeck M, Elsanhoury A, Tschope C, Pieske B, Tauscher G et al. Diagnostic value of cardiovascular magnetic resonance in comparison to endomyocardial biopsy in cardiac amyloidosis: a multi-centre study. CLIN RES CARDIOL. [Journal Article]. 2021 2021-04-01;110(4):555–568
15. Phelan D, Collier P, Thavendiranathan P, Popovic ZB, Hanna M, Plana JC et al. Relative apical sparing of longitudinal strain using two-dimensional speckle-tracking echocardiography is both sensitive and specific for the diagnosis of cardiac amyloidosis. HEART. [Journal Article]. 2012 2012-10-01;98(19):1442–1448
16. Jung HN, Kim SM, Lee JH, Kim Y, Lee S, Jeon E et al (1987) Comparison of tissue tracking assessment by cardiovascular magnetic resonance for cardiac amyloidosis and hypertrophic cardiomyopathy. Acta radiologica 61(7):885–893 2020 2020-01-01
17. Pagourelias ED, Mirea O, Duchenne J, Van Cleemput J, Delforge M, Bogaert J et al. Echo Parameters for Differential Diagnosis in Cardiac Amyloidosis: A Head-to-Head Comparison of Deformation and Nondeformation Parameters. Circulation. Cardiovascular imaging. 2017 2017-01-01;10(3):e5588
18. Mohty D, Boulogne C, Magne J, Varroud-Vial N, Martin S, Ettaif H et al (2016) Prognostic value of left atrial function in systemic light-chain amyloidosis: a cardiac magnetic resonance study. European Heart Journal – Cardiovascular Imaging 17(9):961–969
19. Nochioka K, Quarta CC, Claggett B, Roca GQ, Rapezzi C, Falk RH et al. Left atrial structure and function in cardiac amyloidosis. European heart journal cardiovascular imaging. 2017 2017-01-01;18(10):1128–1137
20. Gregorio CD, Dattilo G, Casale M, Terrizzi A, Donato R, Bella GD. Left Atrial Morphology, Size and Function in Patients With Transthyretin Cardiac Amyloidosis and Primary Hypertrophic Cardiomyopathy– Comparative Strain Imaging Study. Circulation journal : official journal of the Japanese Circulation Society. 2016 2016-01-01;80(8):1830-1837.
21. Rausch K, Scalia GM, Sato K, Edwards N, Lam AK, Platts DG et al (2021) Left atrial strain imaging differentiates cardiac amyloidosis and hypertensive heart disease. Int J Cardiovasc Imaging 37(1):81–90
22. Brand A, Frumkin D, Hübscher A, Dreger H, Stangl K, Baldenhofer G et al (2020) Phasic left atrial strain analysis to discriminate cardiac amyloidosis in patients with unclear thick heart pathology. European Heart Journal - Cardiovascular Imaging. 2020-04-03
23. Elliott PM, Anastasakis A, Borger MA, Borggrefe M, Cecchi F, Charron P et al. 2014 ESC Guidelines on diagnosis and management of hypertrophic cardiomyopathy The Task Force for the Diagnosis and Management of Hypertrophic Cardiomyopathy of the European Society of Cardiology (ESC). EUR HEART J. 2014 2014-01-01;35(39):2733–2779
24. Gersh BJ, Maron BJ, Bonow RO, Dearani JA, Fifer MA, Link MS et al. 2011 ACCF/AHA Guideline for the Diagnosis and Treatment of Hypertrophic Cardiomyopathy: Executive Summary. CIRCULATION. 2011 2011-12-13;124(24):2761–2796

25. Terry KK, Mae YL. A Guideline of Selecting and Reporting Intraclass Correlation Coefficients for Reliability Research. Journal of Chiropractic Medicine. 2016 2016-06-15;15(2)
26. Thomas L, Abhayaratna WP. Left Atrial Reverse Remodeling: Mechanisms, Evaluation, and Clinical Significance. JACC Cardiovasc Imaging. [Journal Article; Review]. 2017 2017-01-01;10(1):65–77
27. Casaclang-Verzosa G, Gersh BJ, Tsang TS. Structural and functional remodeling of the left atrium: clinical and therapeutic implications for atrial fibrillation. J AM COLL CARDIOL. [Journal Article; Research Support, N.I.H., Extramural; Research Support, Non-U.S. Gov't; Review]. 2008 2008-01-01;51(1):1–11

Tables

Table 1. Demographic data and baseline characteristics of subjects.

Parameters	AL (n = 38)	HCM (n = 38)	Control (n=20)	P	P1	P2	P3
Age, year	61.0 ± 9.3	58.9 ± 9.0	57.6 ± 8.4	0.354	-	-	-
Male gender, n (%)	29 (76.3)	24 (63.1)	12 (60.0)	0.334	-	-	-
Heart rate, beats/min	81.5 [71.7, 90.8]	69.6 [64.0, 71.5]	66.0 [61.0, 75.8]	<0.001*	<0.001*	0.001	1
Body mass index, kg/m2	22.5 ± 2.6	24.3 ± 3.1	24.3 ± 3.2	0.010*	0.007*	0.030*	0.934
Systolic blood pressure, mmHg	119.5 ± 22.5	129.0 ± 16.1	115.2 ± 18.3	0.020*	0.034*	0.420	0.011*
Diastolic blood pressure, mmHg	76.6 ± 13.4	82.9 ± 13.8	77.3 ± 9.9	0.083	-	-	-
Sinue rhythm, n (%)	35 (92.1)	36 (94.7)	20 (100.0)	0.629	-	-	-
Cardiac risk factors, n (%)							
Hypertension	10 (26.3)	25 (65.8)	3 (15.0)	<0.001*	0.001*	0.509	<0.001*
Coronary artery disease	1(2.6)	6(15.8)	0 (0.0)	0.070	-	-	-
Diabetes	4(10.5)	11 (28.9)	0 (0.0)	0.009*	0.082	0.288	0.011*
Peak level hs-cTnI, pg/mL	100.0 [23.8, 224.9]	9.2 [5.3, 28.4]	-	<0.001*	-	-	-
NT-proBNP, pg/mL	3816.5 [1222.8, 7508.0]	222.5 [44.0, 540.8]	-	<0.001*	-	-	-
Serum creatinin level, mmol/L	103.0 [81.0, 225.0]	75.5 [67.0, 92.2]	-	0.001*	-	-	-
Glomerular filtration rate, ml/min	63.1 [23.2, 86.1]	84.35 [76.6, 93.8]	-	<0.001*	-	-	-

The values are presented as mean ± standard deviation or number (percentage) or median [interquartle range]. * indicates P < 0.05. - indicates not available. P1 = AL vs. HCM, P2 = AL vs. Control, P3 = HCM vs. Control. hs-cTnI = high-sensitivity troponin I, NT-proBNP = N-terminal pro brain natriuretic peptide, AL = light-chain Amyloidosis, HCM = hypertrophic cardiomyopathy.

Table 2. Left atrial and left ventricular morphological and functional parameters of patients and healthy controls.

Parameters	AL (n = 38)	HCM (n = 38)	Control (n=20)	P	P1	P2	P3
Maximum atrial septal thickness, mm	7.5 ± 2.5	5.0 ± 1.2	4.2 ± 0.9	<0.001*	<0.001*	<0.001*	0.017*
LA volumn index, ml/m²							
Minimum	28.6 [17.0, 40.7]	19.0 [13.9, 26.7]	14.5 [11.3, 16.1]	<0.001*	0.092	<0.001*	0.057
Maximum	45.7 ± 15.1	42.6 ± 13.8	36.2 ± 13.8	0.040*	1.000	0.034*	0.232
Before contraction	38.9 ± 15.5	33.9 ± 13.1	26.9 ± 8.0	0.009*	0.499	0.006*	0.158
LA emptying fraction, %							
Total	37.7 ± 16.3	50.3 ± 11.9	60.1 ± 7.4	<0.001*	0.005*	<0.001*	0.021*
Conduit	16.6 [7.2, 24.1]	21.1 [13.4, 29.0]	27.4 [23.0, 33.7]	0.001*	0.150	0.001*	0.128
Booster	26.6 ± 13.0	37.1 ± 10.8	45.7 ± 7.2	<0.001*	0.003*	<0.001*	0.022*
End-diastolic maximum LV wall thickness, mm	16.1 [13.7, 18.6]	17.3 [16.0, 18.7]	9.9 [8.5, 10.4]	<0.001*	0.530	<0.001*	<0.001*
LV end diastolic volumn index, ml/m²	74.4 [61.0, 88.3]	56.8 [49.6, 66.8]	68.2 [58.3, 81.3]	<0.001*	<0.001*	1.000	0.005*
LV end systolic volumn index, ml/m²	28.3 [24.0, 38.1]	17.9 [15.6, 22.3]	24.4 [19.0, 28.5]	<0.001*	<0.001*	0.335	0.011*
LV ejection fraction, %	60.2 ± 7.2	66.9 ± 6.2	64.3 ± 7.8	<0.001*	<0.001*	0.037*	0.178
Stroke volumn index, ml/m²	46.2 [35.5, 54.2]	35.7 [32.5, 46.1]	40.7 [38.3, 53.1]	0.014*	0.034*	1.000	0.053
Cardiac index, l/min/m²	3.7 ± 1.0	2.7 ± 0.8	3.2 ± 0.9	<0.001*	<0.001*	0.029*	0.068
LV myocardial mass/BSA, g/m²	78.1 ± 22.1	61.1 ± 17.5	43.6 ± 8.0	<0.001*	0.005*	<0.001*	0.001*

The values are presented as mean ± standard deviation or median [interquartle range]. * indicates P < 0.05. - indicates not available. P1 = AL vs. HCM, P2 = AL vs. Control, P3 = HCM vs. Control. LA = left atrium, LV = left ventricle, BSA = body surface area, AL = light-chain Amyloidosis, HCM = hypertrophic cardiomyopathy.

Table 3. Univariate regression analysis of underlying predictors of light-chain amyloidosis.

Parameters	OR	95%CI	P value	AUC
$LAVi_{max}$	1.030	0.998 - 1.062	0.066	-
$LAVi_{min}$	1.066	1.028 - 1.106	0.001*	0.709
$LAVi_{bf}$	1.041	1.009 - 1.074	0.012*	0.646
$LAEF_{total}$	0.922	0.889 - 0.957	<0.001*	0.785
$LAEF_{conduit}$	0.956	0.921 - 0.993	0.019*	0.686
$LAEF_{booster}$	0.908	0.869 - 0.948	<0.001*	0.790
ASH_{max}	2.578	1.723 - 3.858	<0.001*	0.857

* indicates P < 0.05. LAVi = left atrial volume index, min = minimum, LAEF = left atrial emptying fraction, ASH = atrial septal thickness, OR = odds ratio, CI = confidence interval, AUC = area under the curve.

Table 4. Intra- and inter-observer variability of left atrial parameters in randomly selected 20 cases.

	Intra-observer			Inter-observer		
	ICC	95% CI	P value	ICC	95% CI	P value
ASH_{max}	0.973	0.933 - 0.989	<0.001*	0.975	0.939 - 0.990	<0.001*
$LAVi_{min}$	0.936	0.741 - 0.979	<0.001*	0.958	0.899 - 0.983	<0.001*
$LAVi_{max}$	0.925	0.754 - 0.973	<0.001*	0.912	0.749 - 0.967	<0.001*
$LAVi_{bf}$	0.946	0.817 - 0.981	<0.001*	0.944	0.857 - 0.978	<0.001*

* indicates P < 0.05. ASH = atrial septal thickness, LAVi = left atrial volume index, min = minimum, max = maximum, bf = before contraction, ICC = intra-class correlation coefficient, CI = confidence interval.

Figures

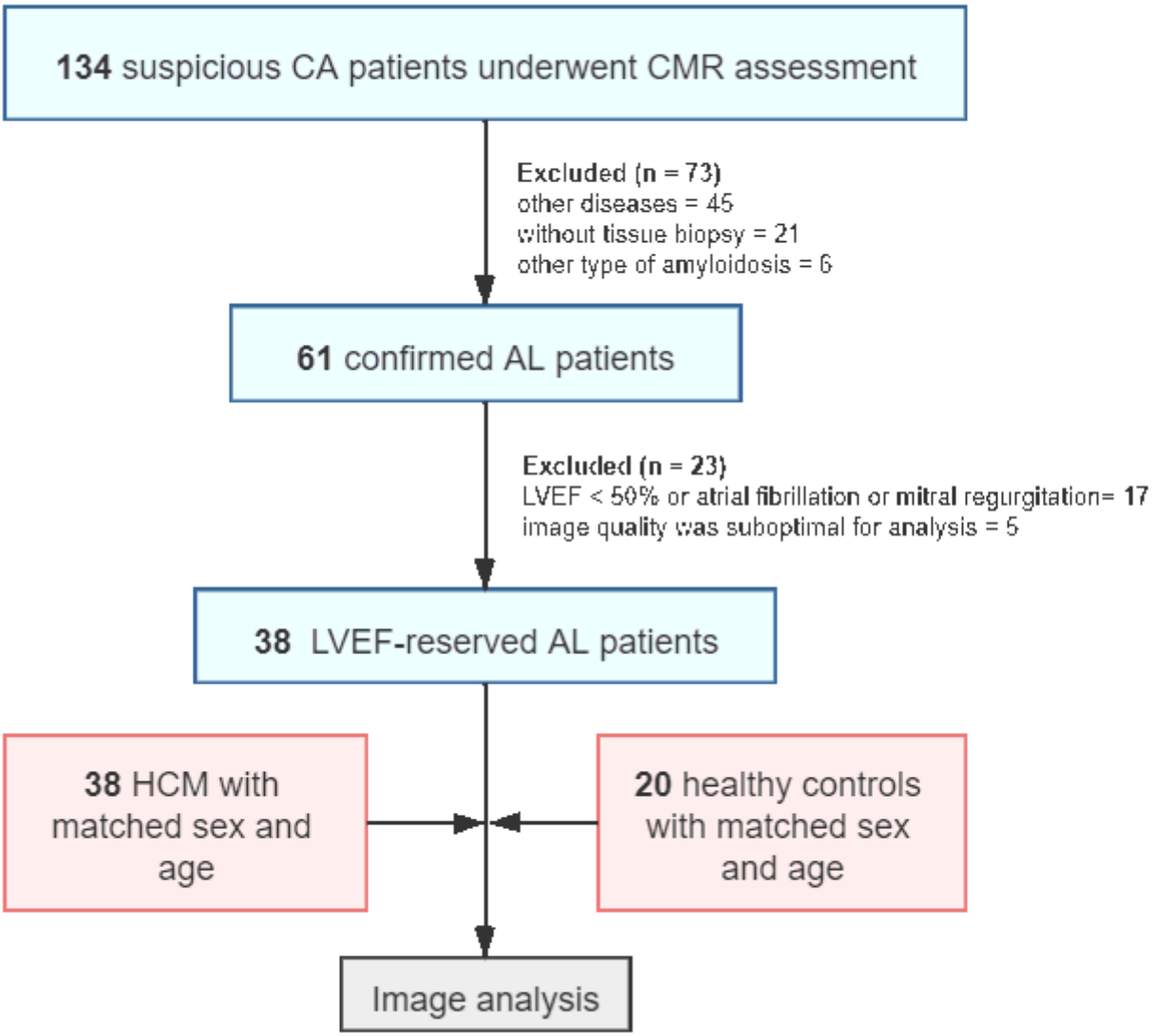

Figure 1

Flow diagram of subjects' inclusion and exclusion. CA = cardiac amyloidosis, CMR = cardiac magnetic resonance, AL = light- chain amyloidosis, LVEF = left ventricular ejection fraction, HCM = hypertrophic cardiomyopathy

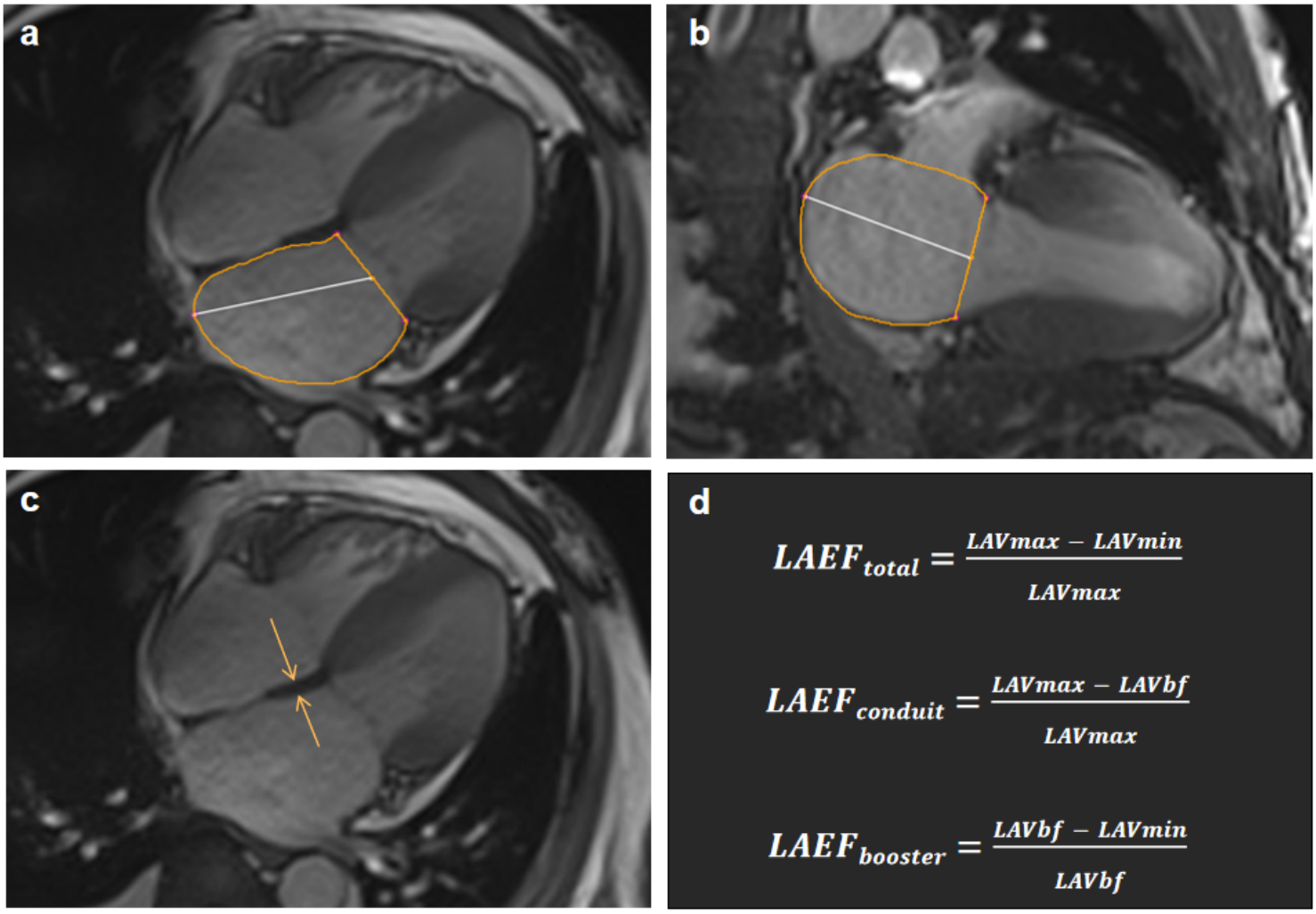

Figure 2

(a, b) Four-chamber and 2-chamber contours of LAV measurements. The LA appendage and pulmonary veins were excluded. (c) Measurement method of atrial septal thickness, which was taken perpendicular to the atrial septum during LA end-diastolic phase. (d) Formulas used for LAEF calculation. LAV = left atrial volume, LAEF = left atrial emptying fraction, max = maximum, min = mnimum, bf = before contraction

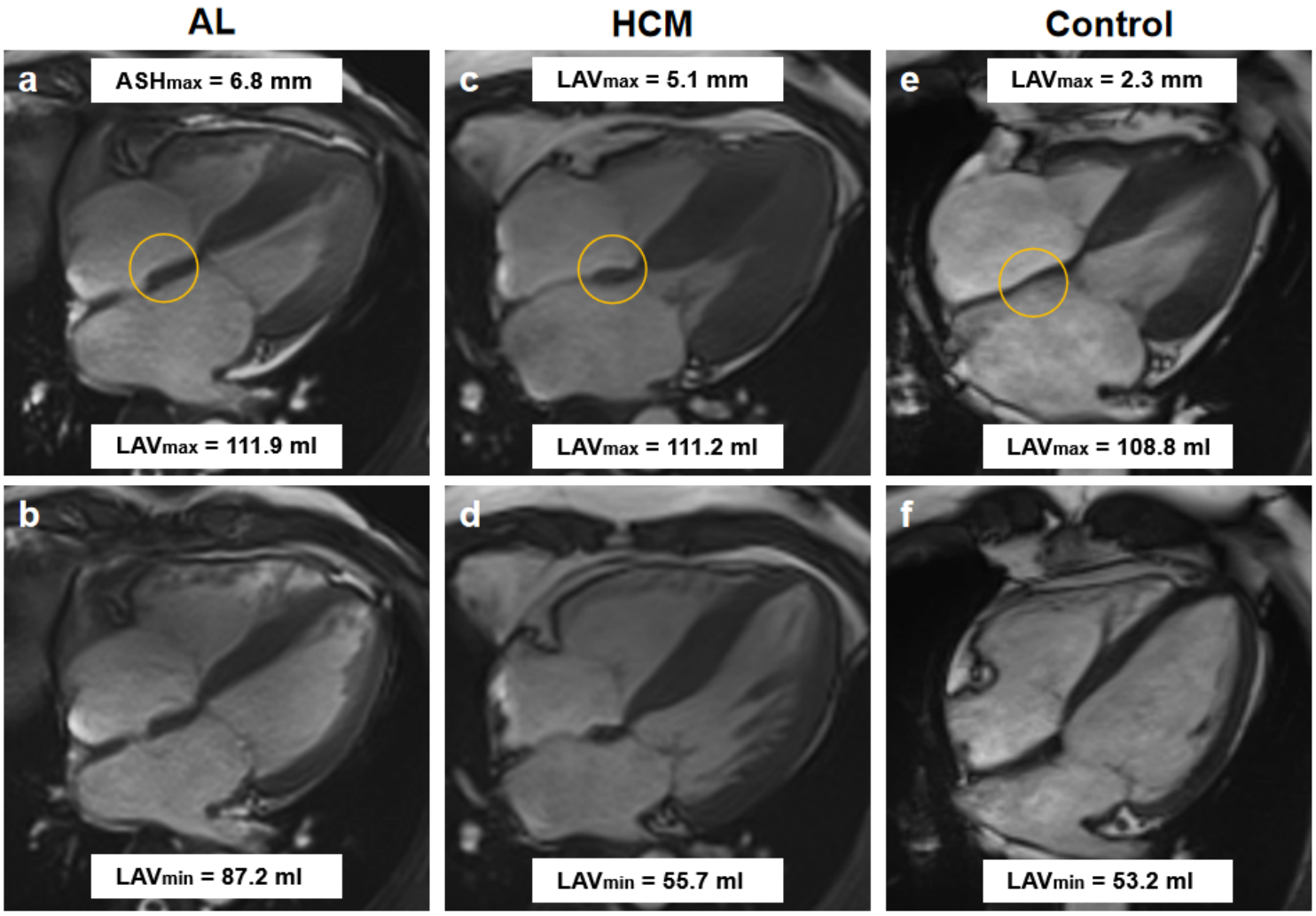

Figure 3

AL patient (a, b), HCM patient (c, d) and control (e, f) showed similar maximum LAV, but the minimum LAV of AL in standard 4-chamber cine image was significantly different from that of HCM and control. And the markedly difference in atrial septal thickness could be seen (orange circle). AL = light-chain amyloidosis, HCM = hypertrophic cardiomyopathy, LAV = left atrial volume

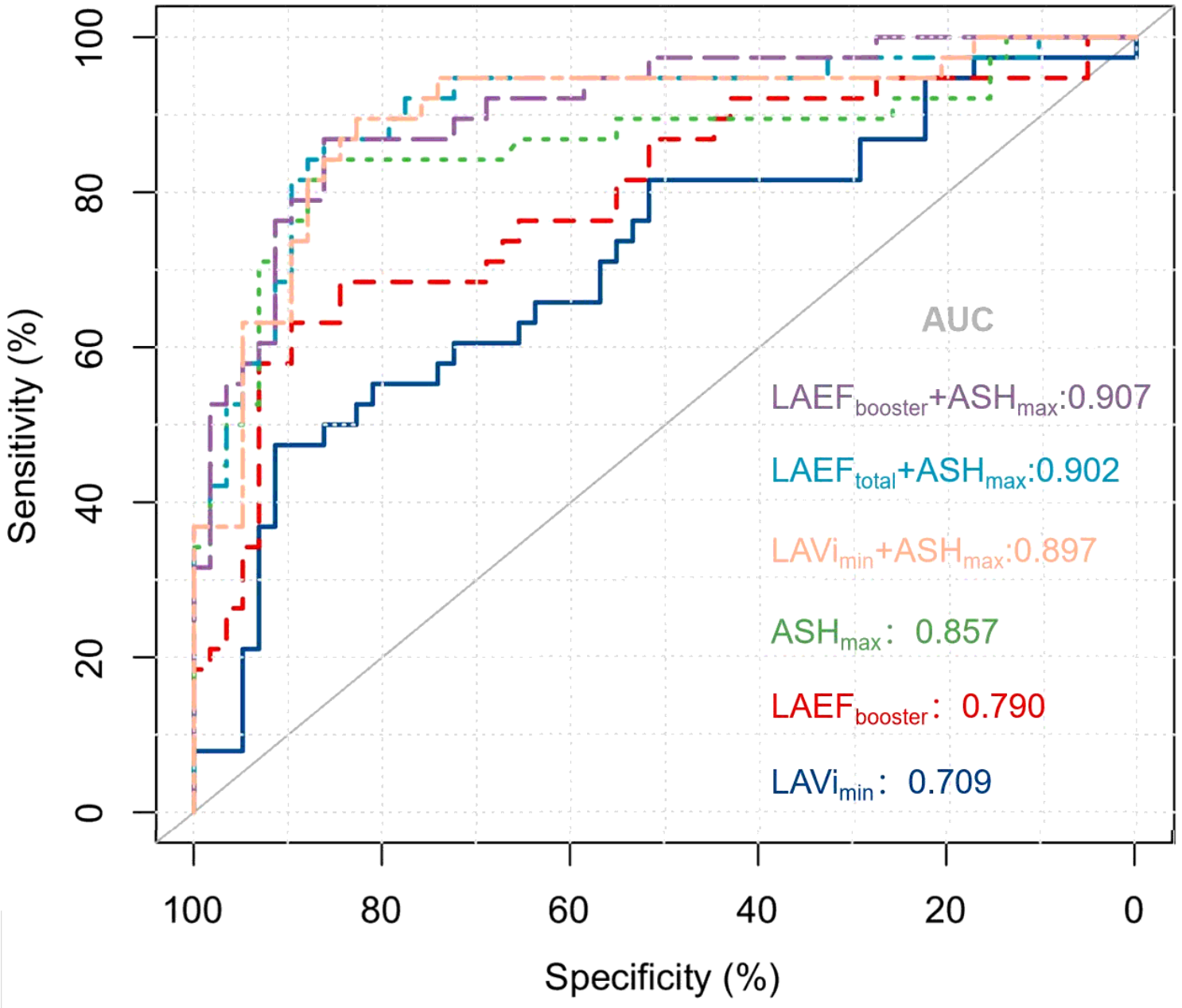

Figure 4

The receiver-operating characteristic curve of CMR-derived LA parameters. AUC = area under the curve, LAEF = left atrial emptying fraction, ASH = atrial septal thickness, LAVi = left atrial volume index